

Intrinsically Switchable Thin Film Ferroelectric Resonators Utilizing Electric Field Induced Piezoelectric Effect

Seyit Ahmet Sis, Victor Lee, Seungku Lee, Amir Mortazawi

The Department of Electrical Engineering and Computer Science at the
University of Michigan, Ann Arbor, Michigan, 48109, USA
Email:sis@umich.edu

Abstract — This paper presents bulk acoustic wave resonators using the ferroelectric materials barium titanate and barium strontium titanate. The electric field induced piezoelectric effect in these materials is utilized in the design of various types of intrinsically switchable bulk acoustic wave resonators. Both thickness mode and lateral mode resonator results, which have been demonstrated recently, are summarized in this paper. Significantly improved quality factors by means of forming a ferroelectric-on-silicon structure are also demonstrated.

Index Terms — Barium strontium titanate, barium titanate, composite FBAR, ferroelectric devices, intrinsically switchable devices, thin film bulk acoustic wave resonators.

I. INTRODUCTION

Frequency selective filter banks are essential components for communication systems and frequency hopping radars [1]. The filter bank in such systems consists of bulk acoustic wave (BAW) or surface acoustic wave (SAW) resonator filters that are connected to RF switches [1].

Recently, ferroelectric based BAW resonators and filters have been demonstrated utilizing the electric field induced piezoelectric effect (electrostrictive effect) in barium titanate (BTO) [2]-[3] and barium strontium titanate (BST) [4]-[8] thin films. Since ferroelectric resonators are intrinsically switchable with the application of a dc bias voltage, ferroelectric BAW filters have the potential for eliminating the necessity of RF switches in filter banks. This makes it possible to significantly decrease the chip area, complexity, and cost.

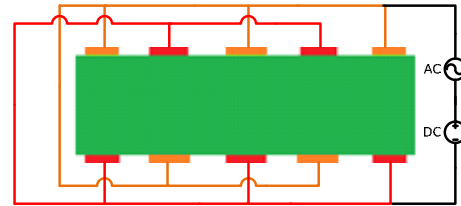
The figures of merit for a filter, such as bandwidth, insertion/return loss and rejection level, strongly depend on the properties of the resonators that make up the filter. For example, the maximum bandwidth of the filter is limited by the electromechanical coupling coefficient of the resonator (K_t^2). Similarly, the insertion loss and the rejection level of the filter are strongly dependent on both the K_t^2 and the quality factor (Q) of the resonator. Furthermore, the Q of the resonators determines the phase noise performance, if these resonators are used in the design of the oscillators. Therefore, researchers have been working on improving the performance of ferroelectric based resonators.

This paper presents the recently-demonstrated thin film ferroelectric based intrinsically switchable resonators. First, lateral mode and thickness mode resonators are discussed. Then, the Q enhancing technique by utilizing a ferroelectric-on-silicon structure is introduced. Fabrication steps of both types of resonators are described afterward. Finally, the measurement results for an interdigitated lateral mode resonator and a high- Q ferroelectric-on-silicon thickness mode resonator are provided.

II. DESIGN PROCEDURE

A. Interdigitated Lateral Mode Resonators

Fig. 1 shows a cross sectional view of an interdigitated lateral mode resonator. The RF signal is connected to the electrodes in an alternating fashion such that neighboring pairs of digits induce the opposite lateral strain. The dc voltage is applied through a bias tee to each opposing pair of electrodes for creating a large static electric field in the ferroelectric layer to induce piezoelectricity.



— Electrodes — Electrodes — Ferroelectric
Fig. 1. Cross-sectional view of an interdigitated lateral mode resonator showing the signal path and biasing configuration.

The resonance frequency of interdigitated lateral mode resonators is mostly determined by the lateral dimensions, such as electrode width and electrode separation, as well as the acoustic properties of the device. Controlling the lateral dimensions is easier and more accurate than controlling the film thicknesses, which is an advantage for lateral mode resonators. This advantage becomes very important when designing a resonator bank or filter bank that requires different resonance frequencies for each

resonator. The equations that are utilized to determine resonance frequency are available in [9].

B. Thickness Mode Resonators

The thin film bulk acoustic wave resonator (FBAR) structure shown in Fig. 2(a) has a sandwiched ferroelectric layer between top and bottom electrodes while a composite FBAR has an additional single-crystal silicon (Si) layer beneath the bottom electrode as seen in Fig. 2(b). The resonance frequencies of both types of FBARs are determined by the thicknesses of the layers [10].

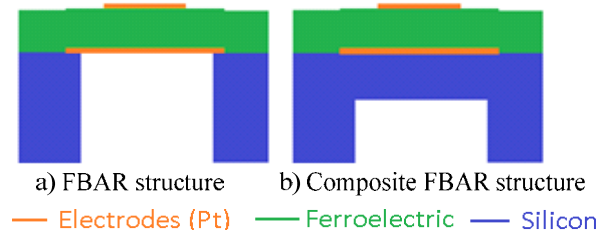


Fig. 2. Cross-sectional view of (a) FBAR (b) composite FBAR.

The composite FBAR structure provides higher quality factors (Q s) as compared to FBARs, thanks to the low acoustic loss of single crystal silicon (Si) [10]. The Si layer also provides additional mechanical support; therefore the yield in fabricated devices is increased. However, the improvement in Q is achieved at the cost of reduced electromechanical coupling coefficient (K_t^2), which is another important figure of merit that represents how well electromechanical transduction occurs. Nevertheless, one can optimize the thickness ratio of ferroelectric layer to silicon layer in order to maximize K_t^2 for a given resonance mode by ensuring that a half wavelength displacement occurs across the ferroelectric layer [10].

III. FABRICATION PROCEDURE

A. Lateral Mode Resonators

The fabrication of lateral mode resonators presented in [3] starts with high resistivity silicon wafer ($\rho \sim 3000 \Omega \cdot \text{cm}$) which has a thickness of $525 \mu\text{m}$. A 100 nm of silicon oxide (SiO_2) is grown on top of the silicon wafer. A 100 nm layer of platinum (Pt), which is used as the bottom electrode, is deposited and patterned by liftoff process using e-beam evaporator deposition and lithography. A 400 nm layer of BTO is deposited using pulsed laser deposition (PLD), details of which are given in [3]. A 100 nm Pt top electrode is patterned by e-beam evaporation and liftoff. The ferroelectric BTO layer is etched by using diluted hydrofluoric (HF) acid to reach the bottom Pt layers for measurement probe contact. The

BTO and SiO_2 layers around the resonator are etched using reactive ion etching to define the lateral dimension of the resonator. A 500 nm gold (Au) contact layer is deposited for the contact pads using e-beam evaporation. Finally, XeF_2 front-side etching technique is used to etch the silicon underneath of the resonator to release it.

B. Composite FBARs

The fabrication of ferroelectric-on-silicon composite FBARs presented in [7] starts with a high resistivity silicon-on-insulator (SOI) wafer which has a $2.5 \mu\text{m}$ thick single crystal Si device layer and $2 \mu\text{m}$ of buried oxide (SiO_2). A 100 nm of Pt layers are then deposited and patterned by evaporation and lift-off. A 300 nm of BST layer is deposited using (PLD). 100 nm of Pt is deposited and patterned by liftoff process using evaporation and lithography. The BST thin film is then etched using diluted HF to create via to reach bottom electrodes. A 500 nm layer of Au is deposited to create probe contact pads. The $400 \mu\text{m}$ thick silicon handling layer underneath of the device is etched by DRIE back-side etching technique.

IV. MEASUREMENT RESULTS

S parameters for both lateral mode and thickness mode resonators are acquired with a vector network analyzer (VNA). The devices are measured on-wafer with $150 \mu\text{m}$ pitch size RF probes on a probe station. The devices are biased through the bias tees connected to input port. The Q and K_t^2 are calculated using

$$Q = \frac{f}{2} \left| \frac{d\phi_{Zin}}{df} \right| \quad (1)$$

and

$$K_t^2 = \frac{\pi}{2} \frac{f_s}{f_p} \tan \left(\frac{\pi}{2} \frac{(f_p - f_s)}{f_p} \right) \quad (2)$$

where ϕ_{Zin} , f_s , and f_p are the phase of the input impedance, series resonance frequency, and parallel resonance frequency, respectively.

A. Lateral Mode Resonator

The photograph of the measured interdigitated lateral mode resonator is shown in Fig. 3. Both electrode width and electrode separation are $1 \mu\text{m}$.

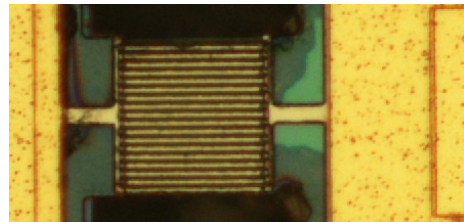


Fig. 3. Photograph of an interdigitated lateral mode resonator.

The input impedance of the measured resonator is shown in Fig. 4 for 0 V and 10 V dc bias voltages. At 0 V, there is no electric field induced piezoelectric effect and therefore the device acts like a capacitor. However, at 10 V dc bias voltage, the electric field induced piezoelectric effect excites acoustic waves, resulting in resonance modes as can be seen in Fig. 4.

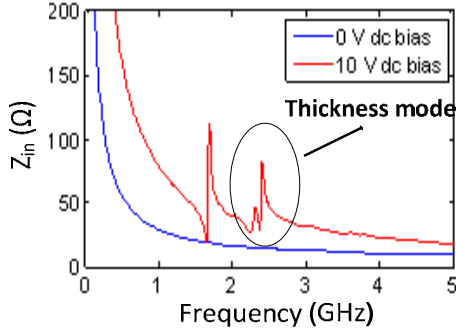


Fig. 4. The input impedance of the lateral mode resonator for 0V and 10 V dc bias voltage.

The Q of the resonator is calculated to be 178 and 152 at the series and parallel resonance frequencies of 1.67 GHz and 1.68 GHz [3], respectively. The K_t^2 of the resonator is calculated to be 2.0 % [3].

B. Composite FBAR

The photograph of the measured composite ferroelectric-on-silicon FBAR is shown in Fig. 5. The input impedance and reflection coefficient of the resonator showing the highest Q resonance mode is shown in Fig. 6 for 0 V, 8V, 12 V and 16 V dc bias voltages. This resonator has BST thickness of 300 nm and total Si and SiO₂ thickness of 4 μm approximately. The electric field induced piezoelectricity ensures the resonator to be intrinsically switched on and off with the application of dc bias voltage.

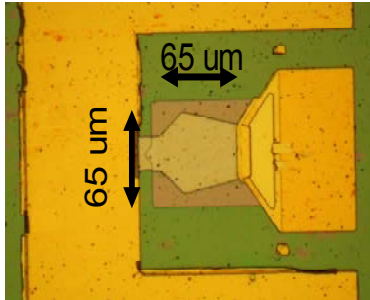


Fig. 5. Photograph of a composite thickness mode resonator.

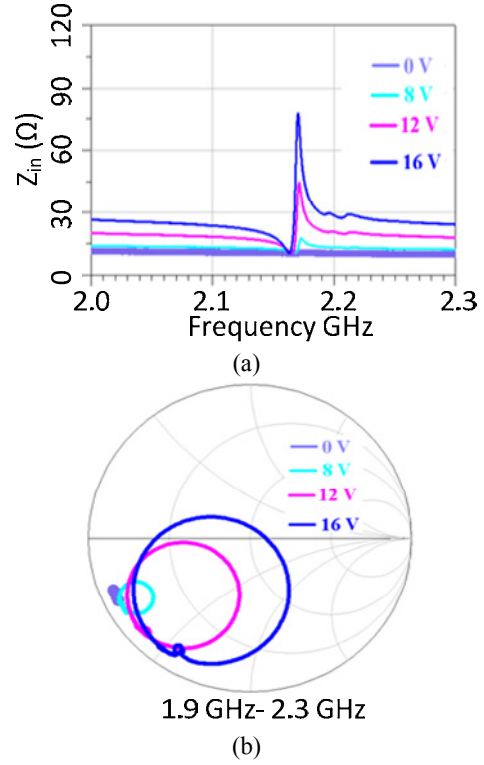


Fig. 6. The measurement results of (a) magnitude of input impedance and (b) reflection coefficient on Smith chart for thickness mode resonator for 0 V, 8 V, 12 V and 16 V dc bias voltages.

The Q s of the resonator are 448 and 617 at the series and parallel resonance frequencies of 2.163 GHz and 2.169 GHz, respectively. The K_t^2 of the resonator is 0.7 % for this resonance mode.

In addition to the results shown above, a recent measurement result of ferroelectric-on-silicon resonator which has 10 μm single crystal silicon layer exhibits Q s in excess of 800 with K_t^2 of 1 %. The results of this resonator are yet to be published.

VII. CONCLUSION

Results of the recently demonstrated lateral mode and thickness mode intrinsically switchable resonators are presented in this paper. The improvement in the Q and yield of FBAR resonators resulting from the composite structure is explained. Efforts in improving the performance of the resonators are ongoing.

ACKNOWLEDGEMENT

Fabrication is performed at the Lurie Nanofabrication Facility, a member of the National Nanotechnology

Infrastructure Network, which is supported in part by the National Science Foundation.

REFERENCES

- [1] Jiangsheng Liu; Shitang He; Shunzhou Li; Jiuling Liu; Yong Liang; , "P6G-3 Switchable SAW Filter Bank with Both Narrow & Wide Channel Bandwidth and 10 Channels SAW Filter Bank," *Ultrasonics Symposium, 2007. IEEE* , vol., no., pp.2578-2581, 28-31 Oct. 2007
- [2] Xinen Zhu; Lee, V.; Phillips, J.; Mortazawi, A.; , "Intrinsically switchable contour mode acoustic wave resonators based on barium titanate thin films," *Microwave Symposium Digest, 2009. MTT '09. IEEE MTT-S International* , vol., no., pp.93-96, 7-12 June 2009
- [3] Lee, V.; Sis, S.A.; Xinen Zhu; Mortazawi, A.; , "Intrinsically switchable interdigitated barium titanate thin film contour mode resonators," *Microwave Symposium Digest (MTT), 2010 IEEE MTT-S International* , vol., no., pp.1448-1450, 23-28 May 2010
- [4] Sis, S.A.; Lee, V.; Mortazawi, A.; , "Intrinsically switchable, BST-on-silicon composite FBARs," *Microwave Symposium Digest (MTT), 2011 IEEE MTT-S International* , vol., no., pp.1-4, 5-10 June 2011
- [5] Xinen Zhu; Phillips, J.D.; Mortazawi, A.; , "A DC Voltage Dependant Switchable Thin Film Bulk Wave Acoustic Resonator Using Ferroelectric Thin Film," *Microwave Symposium, 2007. IEEE/MTT-S International* , vol., no., pp.671-674, 3-8 June 2007
- [6] Sis, Seyit Ahmet; Lee, Victor; Phillips, Jamie D.; Mortazawi, Amir; , "A DC voltage dependent switchable acoustically coupled BAW filter based on BST-on-silicon composite structure," *Microwave Symposium Digest (MTT), 2012 IEEE MTT-S International* , vol., no., pp.1-3, 17-22 June 2012
- [7] Sis, Seyit Ahmet; Lee, Victor; Phillips, Jamie D.; Mortazawi, Amir; , "Intrinsically switchable thin film ferroelectric resonators," *Microwave Symposium Digest (MTT), 2012 IEEE MTT-S International* , vol., no., pp.1-3, 17-22 June 2012
- [8] A. Vorobiev and S. Gevorgian, "Tunable $\text{Ba}_{1-x}\text{Sr}_x\text{TiO}_3$ FBARs based on SiO_2/W Bragg reflectors," in *IEEE MTT-S Int. Microw. Symp. Dig.*, May 2010, pp. 1444-1447
- [9] P. J. Stephanou, A. P. Pisano, "PS-4 GHZ Contour Extensional Mode Aluminum Nitride MEMS Resonators," *Ultrasonics Symposium, 2006. IEEE* , vol., no., pp.2401-2404, 2-6 Oct. 2006
- [10] K. M. Lakin and J. S. Wang, "Acoustic bulk wave composite resonators," *Appl. Phys. Lett.*, vol. 38, no. 3, pp. 125-127, Feb. 1981.